Wahle, K.; Staneva, J.; Guenther, H.:

Data assimilation of ocean wind waves using Neural Networks. A case study for the German Bight

In: Ocean Modelling (2015) Elsevier

DOI: 10.1016/j.ocemod.2015.07.007

Data assimilation of ocean wind waves using Neural Networks. A case study for the German Bight.

Kathrin Wahle[1], Joanna Staneva[1], Heinz Guenther[1]

Helmholtz-Zentrum Geestahcht, Max–Planck–Str. 1, 21502 Geesthacht, Germany

Abstract

A novel approach of data assimilation based on Neural Networks (NN's) is presented and applied to wave modelling in the German Bight. The method takes advantage from the ability of NN's to emulate models and to invert them. Combining forward and inverse model NN with the Levenberg-Marquardt algorithm provides boundary values or wind fields in agreement with measured wave integrated parameters. Synthezised HF-radar wave data are used to test the technique for two academic cases.

Keywords: Neural Networks, inverse modelling, data assimilation, WAM, HF-radar

1. Introduction

Data assimilation (DA) into regional wave models are often hampered due to two reasons: when simple assimilation schemes, such as optimal interpolation, are used the model innovation rapidly decreases. Advanced schemes like Ensemble Kalman Filters (EnKF, Evensen (1994), Evensen (2003)), variational methods (DIMET and Talagrand (1986)), and particle filters (Van Leeuwen (2009)) on the other hand are very time consuming. Data assimilation was first invented for numerical atmospheric and hydrodynamic modelling but nowadays is also standard in third generation wave modelling. Since the pioneering work of Lionello et al. (1992) several advanced schemes have been implemented with regional applications (e.g. Voorrips et al. (1997)).

One of the major goals of DA is to improve the accuracy of the model forecasts by incorporating data from observations through different methodology. Variational methods attempt to find the maximum a posteriori probability by

Email address: kathrin.wahle@hzg.de (Kathrin Wahle)

computation of the cost function gradient and applying optimization methods to search for the cost function maximum. Note that the most common approach is to minimize, for convenience, minus the logarithm of the a posteriori probability. Combined with the common assumption of Gaussian a priori probabilities this leads to a quadratic minimization problem. Kalman filtering takes another approach. The model and observation operators are assumed linear, so that the optimization can be solved analytically. Variational data assimilation systems using adjoint wave models so far suffered from the simplicity of the adjoint. Either errors were introduced due to discretizing the analytical adjoint as in Walker (2006) or the adjoint was based on stationary solutions of the governing equations as in Orzech et al. (2013) and Orzech et al. (2014). Only recently a 4D-VAR system based on SWAN is under development (Veeramony et al. (2014)).

The formulation of the EnKF is quite similar to the 3D-Var method. The main difference is that the static background error covariance is replaced by the sample covariance. This sample covariance is computed from an ensemble of model forecasts in a procedure very similar to Monte Carlo methods. Since data assimilation is often quite computationally demanding many approximations have been proposed, such as Proper Orthogonal Decomposition (POD, Altaf et al. (2009)). Hunt et al. (2007) proposed algorithmic changes to EnKF and suggested that the new scheme should be called the Local Ensemble Transform Kalman Filter (LETKF). LETKF is an advanced data assimilation method, which has been tested with numerical weather prediction (NWP) models, from storm to global scales (Szunyogh et al. (2008)). The method also introduces changes that improve the computational efficiency of the algorithm and adds flexibilities that are beneficial when non-local observations are assimilated (Fertig et al. (2007)). However, high resolution coastal wave models require a further increase of memory by using EnKF/LETKF data assimilation approach, making this method a serious barrier for using it in real operational wave model coastal applications.

Here we present a novel assimilation technique based on Neural Networks (NNs) which combines the computational efficiency of sequential methods with non-locality of Kalman and adjoint methods. In general the NN aims to explore an extensive parallel network of simple elements in order to obtain result in a very short time and, at the same time, with insensitivity to loss and failure of some of the elements of the network. After training NN has a lower computational cost than extended and linear KF, variational method, and particle filter. NNs will be used to emulate the regional wave model

integrated parameters from boundary values and wind fields and also to emulate the inverse. When applied to measured wave data a combination of the forward and inverse NN will provide improved boundary values or wind fields for use in the wave model. The method can thus be summarized as a statistical adjoint method.

NNs have also been used in the context of data assimilation in wave modelling: Zhang et al. (2006) used NN to emulate model errors in order to improve the forecast skill. Zamani et al. (2010) emulated the forward model and coupled it with an Ensemble Kalman Filter. But so far, NNs have not been used for the assimialtion itself.

To explore the feasibility of the assimilation technique we used as a test case the German Bight. The Coastal Observing System for Northern and Arctic Seas (COSYNA) aims at the construction of a long-term observatory for southern North Sea (German Bight). COSYNA integrates near real-time measurements with numerical models in a pre-operational way and provides continuously state estimates and forecasts of the coastal ocean state. Observations consist of in-situ measurements from fixed (piles and buoys) and mobile platforms (FerryBox) as well as of remotely sensed data from shore by HF-radar and from space by satellites. The nested-grid modelling system estimates pre–operationally ocean state variables concerning ocean waves, hydrodynamics and suspended matter in the North Sea and German Bight. The main characteristics of COSYNA however, are the integrated approach of combining observations and numerical modelling by data assimilation. In the future, the system of three HF-radars will also measure wave parameters for the German Bight area. We have thus decided to study additionally the possible impact of assimilation of those high-resolution spatial data into the wave model data. So far, the HF–radar data of surface currents have been analyzed concerning their upscaling potential (Wahle and Stanev (2011)) and data is successfully assimilated in the pre-operational hydrodynamic German Bight model (Stanev et al. (2015)). For a similar regional area - the Liverpool Bay - HF–radar wave data have already be assimilated into a regional wave model using an optimal interpolation (Waters et al. (2013)).

In the following section 2 we will frame the basic idea of the NN method. In section 3 the model set–up is specified. Training and testing of the NNs is described in section 4 and the application of the scheme to two academic test cases follows in section 5. We then summarize our results and give some outlook in 6.

2. Method

In the proposed method, we use Neural Networks to emulate a physical model and its adjoint. Given some measurements $\vec{r}_{\mathrm{m}}$ a first (statistical) estimate of model forcings $\vec{c}$ are derived by NN emulating the adjoint model: $\vec{c}_1 = \mathrm{NN}^{-1}(\vec{r}_{\mathrm{m}})$. Subsequent application of forward NN gives an emulated model output $\vec{r}_1$ error χ_1^2 which can be subsequently minimised using the Levenberg-Marquardt algorithm:

$$\chi_k^2 = (\vec{r_m} - \vec{r_k})^{\mathrm{T}}\, \mathbf{C}\, (\vec{r_m} - \vec{r_k}) \quad (1)$$

$$\vec{c_{k+1}} = \vec{c_k} + (\mathbf{M^T C^{-1} M} + \lambda \mathbf{1})^{-1}\, \mathbf{M^T C^{-1}}\, (\vec{r_m} - \vec{r_k}) \quad (2)$$

where $\mathbf{C}$ is the covariance matrix and $\mathbf{M}$ is the Jacobian matrix with $\mathbf{M} \equiv \left(\frac{\partial \vec{r}(\vec{c})}{\partial \vec{c}}\right)|_{\vec{c}=\vec{c_k}}$. $\lambda \in [0,1]$ is a control parameter allowing to gently adjust between a Gauss-Newton ($\lambda = 0$) and a gradient descent ($\lambda = 1$) scheme.

The combination of emulating forward/inverse models with NNs and applying Levenberg-Marquardt algorithm is not a new idea. It has been used in remote sensing for parameter retrieval and out of scope check (Schiller (2007), Schiller and Krasnopolsky (2001), Krasnopolsky and Schiller (2003)). However, the methodology is novel for data assimilation. Its basic principle is visualised in figure 1.

We use feedforward backpropagation networks. Their characteristics will be described briefly, more details can be found in e.g. Bishop (1995) and Haykin (1999). The NNs are organised in layers: one input layer, one output layer and one or more hidden layers in between. Each layer consists of neurons. The number of neurons in the input and output layer are given by the number of their variables. The number of neurons in the hidden layer(s) is problem specific and its fixation needs some experience. Each neuron in a layer is linked to each neuron in a neighbouring layer by a weight.

The NNs work sequentially: each element of the input vector serves as entry for one of the neurons of the input layer. The output of the first hidden layer is computed by summation of the weighted inputs, shifting it by a bias and applying a nonlinear function (a sigmoid here). The procedure repeats until the output layer is reached where the outcome of each neuron gives one element of the output vector.

Weights and biases are the free parameters of the network. They are fixed during the training phase of the NN by supplying a training dataset consisting of pairs of input vectors and corresponding desired output vectors.

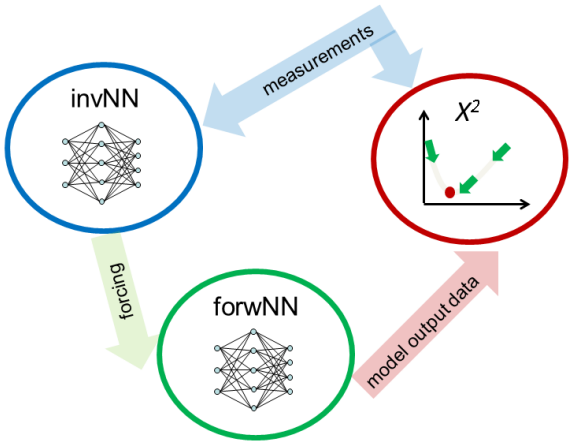

Figure 1: Sketch of assimilation scheme. The combination of forward and backward NN is used to minimize error between measurement and model output.

At the beginning of the training, the outcome of the NN will differ largely from the desired output. The mean squared relative error per neuron is iteratively minimized during the training by backpropagating it through the NN and adjusting the biases and weights according to a gradient descent scheme. This back propagation of errors is also exploited in the Levenberg-Marquardt algorithm: the first guess model output data $\vec{r}_0$ are adapted to better suit the measurements $\vec{r}_\mathrm{m}$.

It is good practice to have an additional independent testing dataset to check the generalization–power of the NN after the training, *i.e.* to test if reasonable output is produced for input not included in the training.

The training and testing phase of the NN methodology is time consuming. However, it needs to be done only once, whereas the subsequent usage of a NN is very fast.

3. Model Set-up

Within COSYNA WAM Cycle 4.5.4 runs pre–operationally twice a day with a three day forecast period. The model is an update of the WAM Cycle

4 wave model, which is described Komen et al. (1996). The basic physics and numerics are kept in the new release. The source function integration scheme of Hersbach and Janssen (1999), and the reformulated dissipation source function (Bidlot et al. (2007),Janssen (2008)) are incorporated. Depth induced wave breaking (Battjes and Janssen (1978)) has been included as an additional source term which will improve model results in shallow areas like the German Wadden Sea.

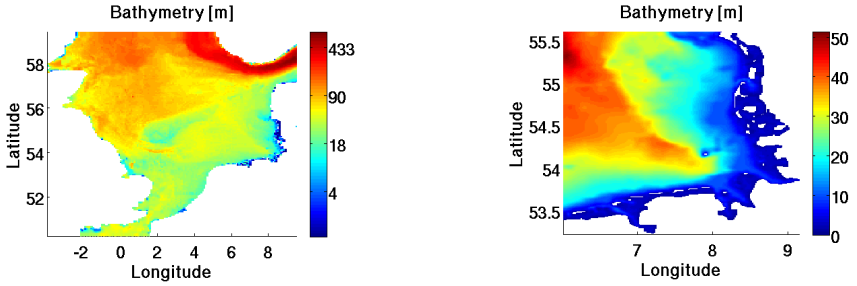

Figure 2: Bathymetry of the North Sea (left) and German Bight model set-up. Note the different scales and the very shallow areas in the German Bight Wadden Sea.

The nested-grid wave model system for the German Bight includes a regional model for the North Sea with a spatial resolution of about 5 km and a finer local model for the German Bight with a resolution of about 900 m. The temporal resolution of integrated wave parameter model output is 3 hours and 1 hour, respectively. Figure 2 shows the depth distributions for both domains. Both models use a directional resolution of 15 degrees and 30 frequencies logarithmically equally spaced from 0.04 Hz to 0.66 Hz. The German Bight model runs include depth refraction and depth induced breaking. The forcing wind fields are taken from the German Met Service (DWD: Deutscher Wetterdienst), computed as U10–fields by the atmospheric model COSMO–EU (Baldauf et al. (2011)). It provides twice a day (0 and 12 UTC) forecast results for 78 hours with a spatial resolution of about 7 km and a temporal resolution of 3 hours. The required boundary information used at the open boundaries of the North Sea model is derived from the regional wave model EWAM for Europe that is running twice a day in the operational wave forecast routine of the DWD.

4. Training Neural Networks

The success of training any NN is highly dependent on the quality of the training data. It has to cover all possible situations equally well. If calm sea state is over represented (as it is in nature) the NN will fail under stormy conditions. Thus, the German Bight model output was sampled for a ten month period starting September 1st 2012. At each time step the 'measurement' region (i.e. where in future HF–radar wave data will be available) was sampled randomly and approximately 20% of the maximum available number has usually been retained. Large values of significant wave height (three times higher than mean at any given point) were always kept and even duplicated.

To reduce the dimensionality of the problem a principal component (PC) analysis for corresponding wind fields and boundary values of significant wave height Hs was performed. In either case the first PC describes well above 90% of the variance (see table 1). Therefore we took the first 2 PCs into account.

# PC	wind U	wind V	Hs N.B.	h_s W.B.
1	93.2	91.0	96.1	95.4
2	3.5 (96.7)	4.1 (95.2)	3.6 (99.7)	3.7 (99.1)
3	1.1 (97.8)	1.9 (97.0)	0.2 (99.9)	0.6 (99.7)
4	0.5 (98.4)	0.7 (97.8)		
5	0.3 (98.7)	0.4 (98.1)		

Table 1: Described variance [%] of leading principal components for wind fields (U and V component) and (northern and western) boundary values of significant wave height Hs in the German Bight. The values in brackets give accumulated values.

In this way a large training / testing table was compiled containing the variables listed in table 2.

Wave period and wave direction at the open boundaries of the German Bight do not vary much with space; therefore information of tm1 and thq was kept in the data table as mean value over boundaries and no PC analysis was done for these variables. The wave travelling time through the German Bight area varies between 6 to 12 hours. Therefore in order to predict present wave heights in the 'measurement' region past 6-12 hours of wind and boundary values are fully relevant. From the large database a subset of approximately

#	variable	time [hours from data]
1	date [YYYYMMDDHH]	
2	longitude of measurement	
3	latitude of measurement	
4	significant wave height Hs	0, -3, -6
5	first moment wave period Tm1	0, -3, -6
6	total mean wave direction θ	0, -3, -6
7	northern boundary Hs PC1/2 and tm1	0, -3, -6, -9, -12
8	northern boundary θ	-6
9	western boundary Hs PC1/2 and Tm1	0, -3, -6, -9, -12
10	western boundary θ	-6
11	wind U/V component PC1/2	0, -3, -6, -9, -12

Table 2: Variables extracted from wave model results for training the various NN's.

90% (>600,000) was randomly chosen for training the various NNs. The remaining 10% (75,000) was used as an independent testing data set.

For training the neural network the method of Schiller (2000) was used.

4.1. NN Forward model

Input to the Neural Network emulating WAM is the northern and western boundary values (first two PC's of Hs, Tm1 period and wave direction θ) reaching 3 to 12 hours back in time, wind (first two PC'a of U- and V component) reaching 0 to 12 hours back in time. Output is the measured wave integrated parameters (Hs, Tm1, θ) at one single location within the measurement area at present time and reaching up to 6 hours back in time. The location of the measurement is defined by its longitude and latitude and given as additional input parameter to the NN. Thus one can interpret the NN as an assembly of NN's – one for each location where observational data might be available.

The reason to train NN's with measurements from only one location at a time and not with all available is twofold: first, NN cannot handle missing values and the HF-radar spatial coverage varies from measurement to measurement. Second, later on in the application phase, the boundary values and wind fields leading to the smallest error $\chi^2 = (\mathrm{Hs_m} - \mathrm{Hs_{NN}})^2/{\mathrm{Hs_m}}^2$ can easily be chosen. A typical distribution of relative errors χ is shown in figure 3.

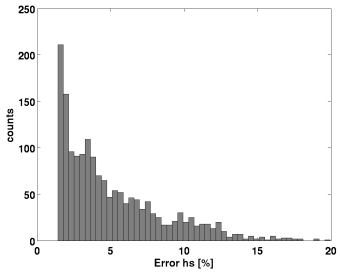

Figure 3: Typical error distribution of all NN ensemble members.

After training the NN its generalisation power was checked relative to the independent testing data set. The statistics of this test are shown in Figure 4 for Hs, Tm1 (t=0) for all points in the testing set. Figure 5 gives the mean spatial distribution of absolute and relative errors for both variables together with the corresponding mean values. Scatterplots of observed versus emulated values demonstrate the performance of the NN. For high values of wave height and period the NN tends to underestimate. In most parts of the German Bight the mean absolute errors are below 20cm and 1/3s corresponding to about 15% and 10%, respectively. In the very shallow areas of the German Bight these values are exceeded by far. This can be explained by considering that during the training of the NN the overall error is minimised by converging to a function that gives small errors in most of the cases. This function is thus similar to the deep water equations of the wave model and thus fails in regions where shallow water physics should be applied. As a consequence measurements taken at these points will not be used for deriving boundary values and wind fields.

4.2. NN Inverse model

As a first attempt we performed the exact inverse of what is described in Section 4.1 for the forward WAM NN, i.e. emulating the boundary forcing from a single point measurement of wave integrated parameters.

However, the results from this inverse NN showed errors that are of one order of magnitude larger than the corresponding forward NN experiment. These large errors were explained by the non-bijectivity of a wave model: one and the same sea state might have been caused by different combinations of swell and wind sea. Thus we decided to reduce the complexity of the inversion problem by dividing the inverse model into two parts: one for

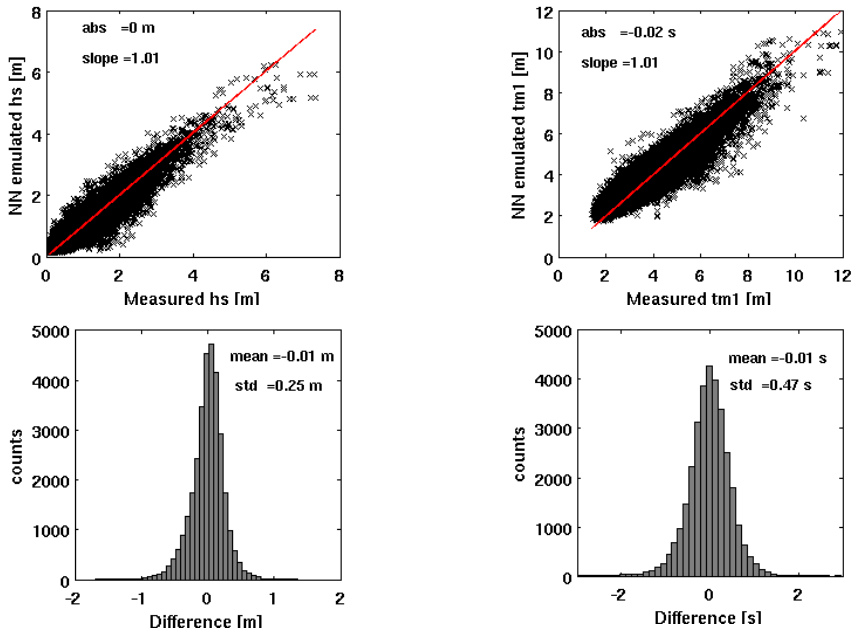

Figure 4: Performance of forward WAM NN when applied to test data. Left: significant wave height, right: tm1 period. The upper figures show a scatterplot of all test data (measured vs. NN emulated) and the best fitted line (with slope and axis intercept). Below, the distribution of deviations (measured minus NN emulated) is given together with the mean of the deviations (bias) and the standard deviation.

deriving boundary values where PC's of wind fields serve as additional input for the inverse NN and a second working vice versa. In this way we thereby improve the inverse NN performance by giving additional input information to the NN.

The splitting might seem unrealistic but it is applicable to many regions. E.g. for most parts of the German Bight correct boundary values are essential for wave forecasting, whereas other regions like the Baltic Sea (not exposed to swell) are dominated by local wind.

4.2.1. Boundary Value retrieval

Figure 6 shows the errors of the inverse WAM NN for boundary value retrieval when wind information was given as an additional input using the example of boundary values 6 hours before the measurement. The performance of this experiment is considerably improved compared to the complete inverse NN. The NN emulated PC's of boundary data of Hs fit the target

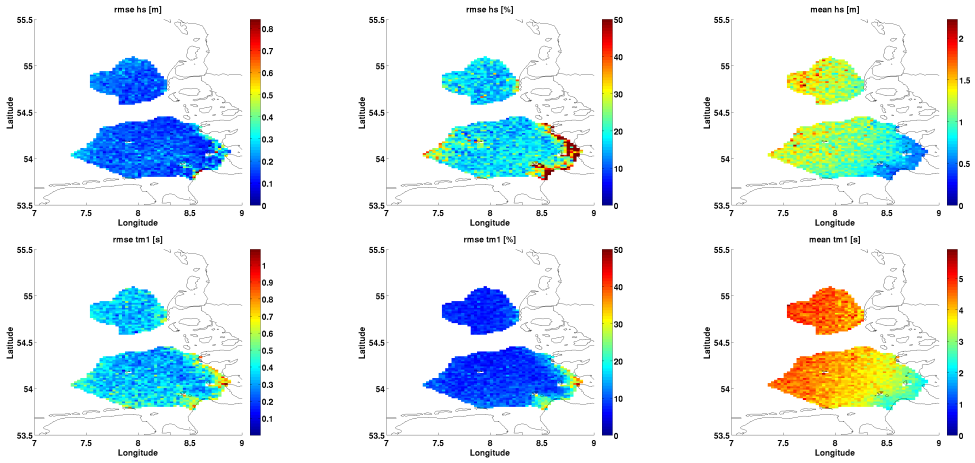

Figure 5: Spatial distribution of mean errors of forward WAM NN when applied to test data. Top: significant wave height, bottom: tm1 period. Left panel shows absolute errors, in the middle are relative errors. Additionally, to the right the mean states are given.

values well. There is a trend of overpredicting by the NN, especially for very small values of the leading PC's which results in an underestimation of large values of significant wave height by the NN.

4.2.2. Wind field retrieval

The NN for wind field retrieval from wave measurements and boundary values shows a broad distribution of errors. As an example Figure 7 shows the first PC's of the wind components 6 hours before measurement for the test data set. When scaled equally the standard deviation here exceeds the corresponding one of the NN emulating boundary values by a factor of 1.5. This might be explained by the fact that the described variance of the leading PC's for the wind field are about 5% less than for boundary values. Additionally, for the northern component there is a small bias.

5. Application of assimilation scheme

In order to test the assimilation scheme two academic tests were performed. Data from the pre- operational wave forecast system for the German Bight area served as synthetic HF-radar data to be assimilated. These data were neither used for training or testing the various NN's and cover the second week of July 2013. The wind fields and boundary values of this forecast

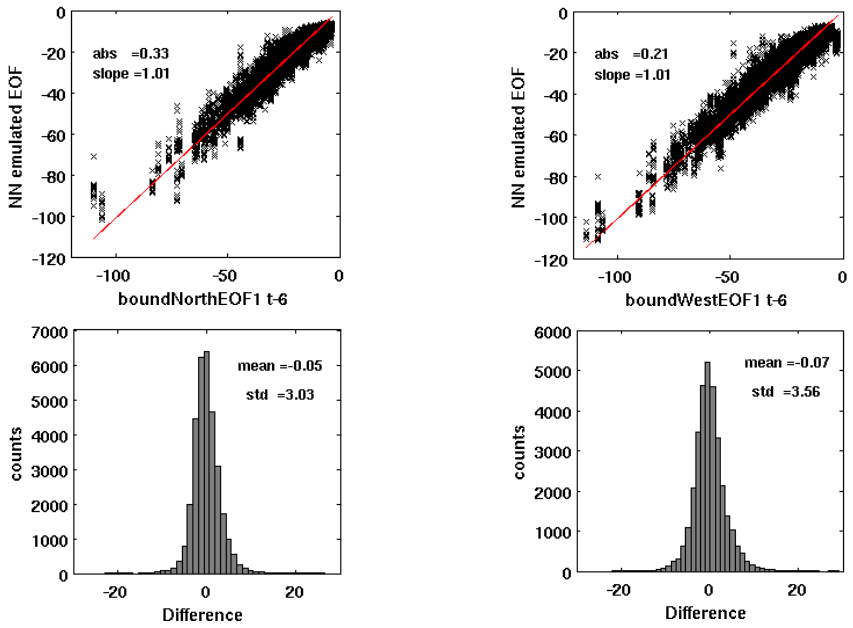

Figure 6: Performance of NN for boundary value retrieval when applied to test data. Left: leading PC of northern boundary Hs 6 hours before measurement, right: same for western boundary. The upper figures show a scatterplot of all test data (measured vs. NN emulated) and the best fitted line (with slope and axis intercept). Below, the distribution of deviations (measured minus NN emulated) is given together with the mean of the deviations (bias) and the standard deviation.

are used for validation of the assimilation. The forecast was re-run to obtain first-guess values using the following to setups:

1. using the correct wind fields but no boundary values
2. using the correct boundary values but no wind

The synthetic HF-radar data together with (1) correct PC's of wind-fields or (2) correct PC's of boundary data were applied to the two NN's emulating the inverse WAM. The NN output (either innovated wind fields or boundary values) was optimized using the Levenberg-Marquardt algorithm described in section 2 and by taking the mean of the 50 outputs giving the smallest error χ^2. Figures 8 and 9 show a comparison between NN output and the correct values. The emulated boundary values agree on the main line with the correct values over the whole assimilation period. The storm event (around 60 hours) is underestimated by about 60 cm and reaches too far south at

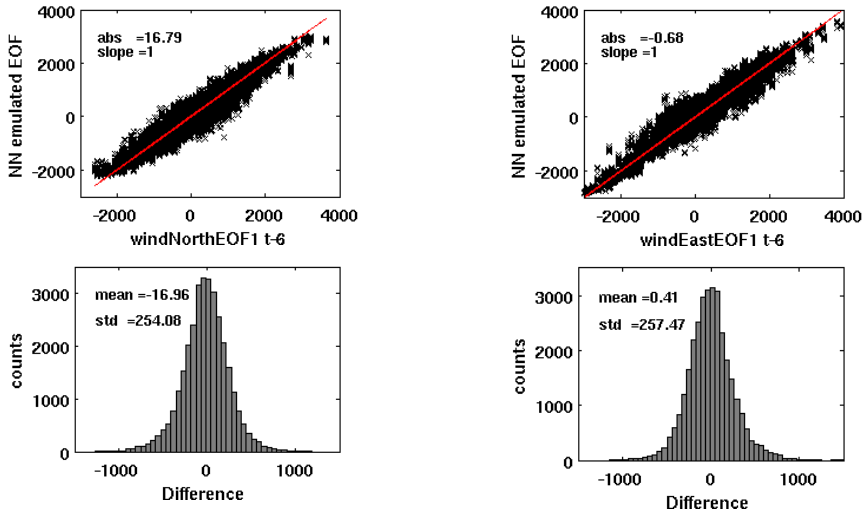

Figure 7: Performance of NN for wind field retrieval when applied to test data. Left: leading PC of wind vector V–component 6 hours before measurement, right: same for U–component. (For details see Figure 6.)

the western boundary. Afterwards emulated Hs drops too rapidly. The wind fields emulated by the NN resembles the model values along the two transects. The wind speed during the storm is underestimated up to 3 m/s towards the northern open boundary and the east coast. In addition, the storm duration is underestimated. Emulated wind directions are mainly northern, whereas the correct wind fields contain an east component. Still, the overall performance of the inverse NN for wind retrieval is encouraging.

For further testing, the emulated wind fields and boundary values were used together with either correct boundary values or correct wind fields as input to the NN emulating WAM. The obtained wave heights and periods give an estimate of innovations that could be achieved in WAM. Figures 10 and 11 show the time averaged relative errors in the area where data were assimilated. Evidently, first-guess errors are largest in the open sea area when boundary values are neglected and largest towards the coast when suppressing wind fields, since the shallow wave state is dominated by local wind. The errors of the innovated wave parameters is reduced significantly (about 20%) in either case throughout most of the measurement area in particular for Tm1 wave period. Close to the East coast the errors exceed the first guess errors by far. This can be explained by the fact, that the NN

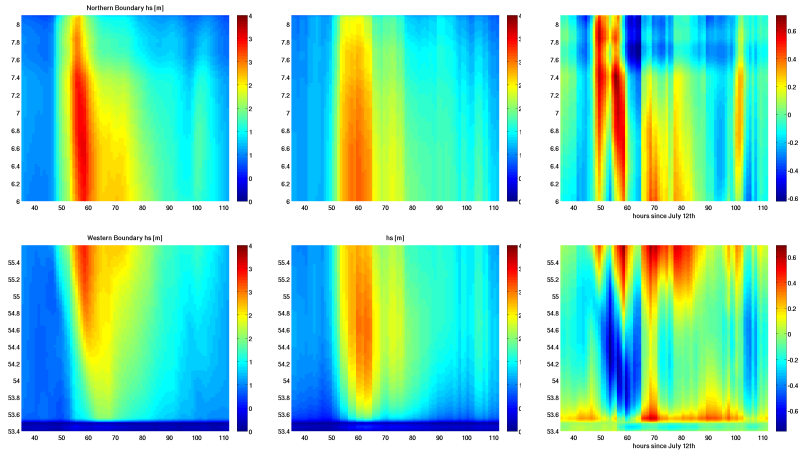

Figure 8: Boundary values taken from WAM model run (left) and as emulated by Neural Network based assimilation scheme (middle) and the difference between the two (WAM-NN). Top: significant wave height at Northern boundary, bottom: at Western boundary. The x–axis is hours since July 12th 12 UTC, y–axis is either longitude or latitude.

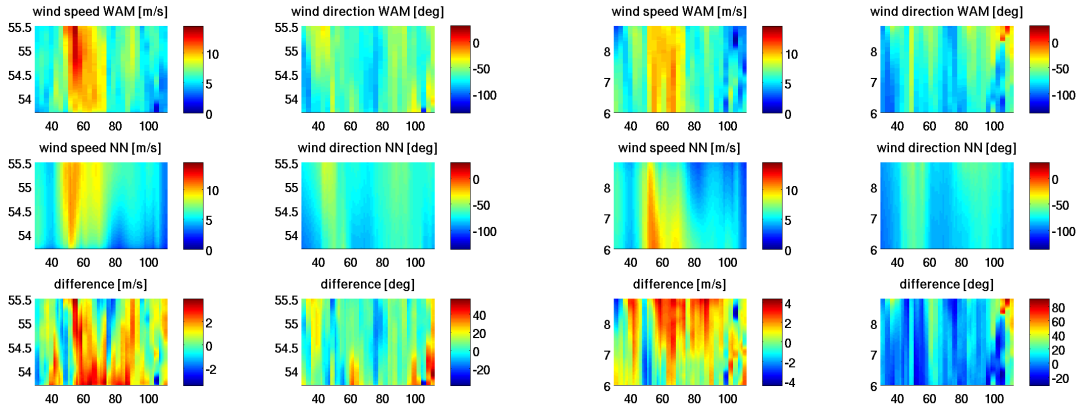

Figure 9: Wind fields (wind speed and direction) taken from WAM model run (top) and as emulated by Neural Network based assimilation scheme (below) and the difference between the two (WAM-NN). Left: profiles along 8 degrees East, right: profiles along 54 degrees North in the German Bight area.

emulating WAM is performing weakest in that area (see section 4.1) due to shallow water effects.

In summary, the first validation of the assimilation scheme gives promising results in the open ocean. It can be supposed that running WAM with NN derived forcing the large errors in the shallow regions will be diminished.

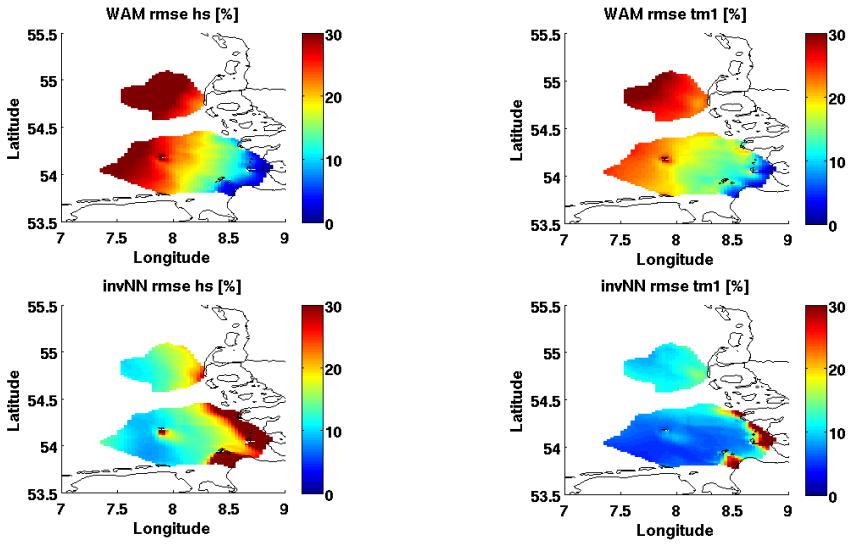

Figure 10: Time averaged relative errors for significant wave height (left) and m1 period (right). The first guess WAM model run (no boundary values) is on top and below innovations as emulated by Neural Network using correct wind fields and boundary values from assimilation scheme.

6. Summary

In this work we used a neural networks (NN) approach as a novel method for data assimilation into a wave model. The method is based on emulating the wave model and its inverse using NN's. By applying wave measurements to them, innovated boundary values and wind fields were retrieved using an iterative process. The potential innovations when using these forcings were estimated using the forward NN.

NN can be used to approximate an arbitrary non-linear function that maps a vector of input variables to a vector of output variables. The application of a NN has been divided into a training phase and a forecasting phase. During the training phase a large dataset of input and output vectors are used to train the NN, i.e. to estimate the coefficients and structure of the

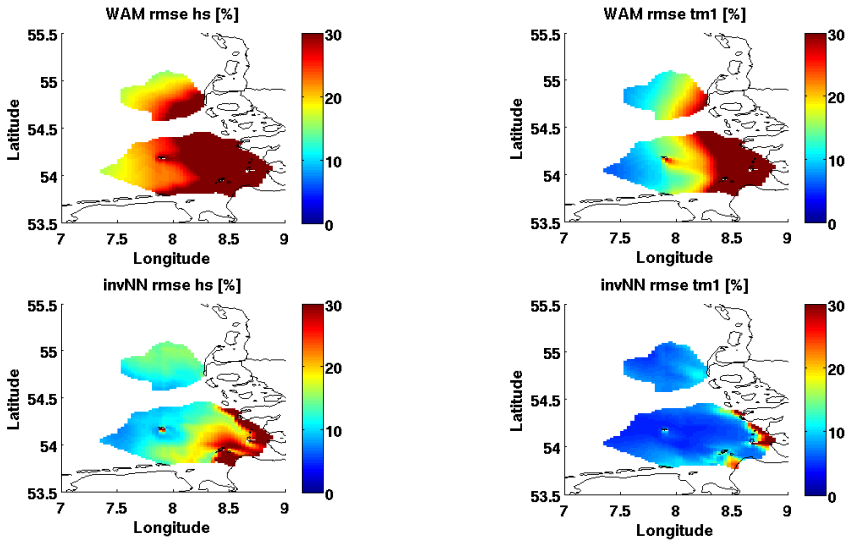

Figure 11: Same as Figure 10 but with first guess WAM model run without wind fields and innovations as emulated by Neural Network using correct boundary values and wind fields from assimilation scheme.

NN. The training phase consists of adjusting the weights for the best performance of the network in establishing the mapping of many input/output vector pairs.

Contrary to physically based models, with the NN it is not necessary that the relation between inputs and outputs is causal, a statistical relation like correlation is sufficient. This gives an additional freedom to decide which variables are inputs and which variables are outputs. This unique property of NN makes possible to perform data-assimilation by simply changing the input and output variables for the NN. Where physically based wave models, such as WAM, require wind and boundary conditions as inputs and provide computed wave parameters on the grid-points as outputs, a NN can accept observed wave parameters as inputs and wind and boundary conditions as outputs. The technical changes for this are very small. The challenge of this method is to select the right input and output variables that work well, since a NN will always provide an answer, but some choices can result in much more accurate results than others.

To understand the performance of NNs for data assimilation in wave models it is difficult to estimate both wind and boundary conditions together. Therefore we used the new methodology either for optimizing the wind forc-

ing or the boundary conditions. We demonstrated here that NNs provide a statistical estimation procedure and thus have similar properties to e.g. multiple linear regression methods. For example, if too many input variables are selected, with a limited set of training data, then the training may overfit the data. It was therefore necessary to reserve part of the available data for validation. The most obvious indication for over-fitting is when the NN has a much higher accuracy for the training data than for the validation data. An important technique to reduce over-fitting is to reduce the number of inputs. We demonstrated that one way to do this is with Principal Component Analysis (PCA), sometimes also called POD, POP or EOF. Another way was to lump a variable e.g. for a whole boundary instead of allowing spatial variation.

A NN is sometimes trained for each scalar output variable separately. This makes it cumbersome to compute output for many output variables. The approach proposed here was to use an 'inverse' NN to estimate the wave parameters at the open boundary of the wave model from the observations. These estimated boundary conditions were used as input for a run with a physically based model, here WAM. It has been also possible to train a forward NN to generate output for a limited number of output locations.

In summary, the results of the twin experiments are very promising and confirm the practicability of the newly developed assimilation technique. The method has several advantages compared with other methods: it can be easily implemented for other wave models and regions since it only requires model output and measurements. Additionally, it can be adapted to specific problems (derive improved wind fields and/or boundary conditions or any other model parameter of interest). Data Assimilation using Neural Networks is computational very efficient compared to other advanced (non-local) assimilation strategies.

7. Acknowledgement

The research leading to the described results was funded by the European Community's Seventh Framework Programme under grant agreement 284455 (MyWave project).

8. References

Altaf, M. U., Heemink, A. W., Verlaan, M., 2009. Inverse shallow-water flow modeling using model reduction. International journal for multiscale

computational engineering 7 (6).

Baldauf, M., Seifert, A., Förstner, J., Majewski, D., Raschendorfer, M., Reinhardt, T., 2011. Operational convective-scale numerical weather prediction with the cosmo model: description and sensitivities. Monthly Weather Review 139 (12), 3887–3905.

Battjes, J., Janssen, J., 1978. Energy loss and set-up due to breaking of random waves. Coastal Engineering Proceedings 1 (16).

Bidlot, J., Janssen, P., Abdalla, S., 2007. A revised formulation of ocean wave dissipation and its model impact. Tech. Rep. 509, ECMWF, Reading, UK, Tech. Memo, available online at: http://www.ecmwf.int/publications/.

Bishop, C., M., 1995. Neural Networks for Pattern Recognition. Clarendon Press, Oxford.

DIMET, F.-X. L., Talagrand, O., 1986. Variational algorithms for analysis and assimilation of meteorological observations: theoretical aspects. Tellus A 38 (2), 97–110.

Evensen, G., 1994. Sequential data assimilation with a nonlinear quasi-geostrophic model using monte carlo methods to forecast error statistics. Journal of Geophysical Research: Oceans (1978–2012) 99 (C5), 10143–10162.

Evensen, G., 2003. The ensemble kalman filter: Theoretical formulation and practical implementation. Ocean dynamics 53 (4), 343–367.

Fertig, E. J., Hunt, B. R., Ott, E., Szunyogh, I., 2007. Assimilating non-local observations with a local ensemble kalman filter. Tellus A 59 (5), 719–730.

Haykin, S., 1999. Neural Networks, A Comprehensive Foundation. Prentice–Hall, Inc., New Jersey.

Hersbach, H., Janssen, P., 1999. Improvement of the short-fetch behavior in the wave ocean model (wam). Journal of Atmospheric and Oceanic Technology 16 (7), 884–892.

Hunt, B. R., Kostelich, E. J., Szunyogh, I., 2007. Efficient data assimilation for spatiotemporal chaos: A local ensemble transform kalman filter. Physica D: Nonlinear Phenomena 230 (1), 112–126.

Janssen, P. A., 2008. Progress in ocean wave forecasting. Journal of Computational Physics 227 (7), 3572–3594.

Komen, G. J., Cavaleri, L., Donelan, M., Hasselmann, K., Hasselmann, S., Janssen, P., 1996. Dynamics and modelling of ocean waves. Cambridge university press.

Krasnopolsky, V., Schiller, H., 2003. Some neural network applications in environmental sciences part i: Forward and inverse problems in geophysical remote measurements. Neural Networks 16, 321–334.

Lionello, P., Günther, H., Janssen, P. A., 1992. Assimilation of altimeter data in a global third-generation wave model. Journal of Geophysical Research: Oceans (1978–2012) 97 (C9), 14453–14474.

Orzech, M., Veeramony, J., Flampouris, S., 2014. Optimizing spectral wave estimates with adjoint-based sensitivity maps. Ocean Dynamics 64 (4), 487–505.

Orzech, M. D., Veeramony, J., Ngodock, H., 2013. A variational assimilation system for nearshore wave modeling. Journal of Atmospheric and Oceanic Technology 30 (5), 953–970.

Schiller, H., 2000. Feedforward–backpropagation neural net program ffbp1.0. GKSS–report 2000/37, iSSN 0344–9629.

Schiller, H., 2007. Model inversion by parameter fit using nn emulating the forward model – evaluation of indirect measurements. Neural networks 20 (4), 479–483.

Schiller, H., Krasnopolsky, V., 2001. Domain check for input to nn emulating an inverse mode. In: International joint conference on neural networks. p. 21502152.

Stanev, E., Ziemer, F., Schulz-Stellenfleth, J., Seemann, J., Staneva, J., Gurgel, K.-W., 2015. Blending surface currents from hf radar observations and numerical modeling: Tidal hindcasts and forecasts. Journal of Atmospheric and Oceanic Technology 32 (2), 256–281.

Szunyogh, I., Kostelich, E. J., Gyarmati, G., Kalnay, E., Hunt, B. R., Ott, E., Satterfield, E., Yorke, J. A., 2008. A local ensemble transform kalman

filter data assimilation system for the ncep global model. Tellus A 60 (1), 113–130.

Van Leeuwen, P. J., 2009. Particle filtering in geophysical systems. Monthly Weather Review 137 (12), 4089–4114.

Veeramony, J., Orzech, M. D., Edwards, K. L., Gilligan, M., Choi, J., Terrill, E., De Paolo, T., 2014. Navy nearshore ocean prediction systems. Tech. rep., DTIC Document.

Voorrips, A., Makin, V., Hasselmann, S., 1997. Assimilation of wave spectra from pitch-and-roll buoys in a north sea wave model. Journal of Geophysical Research: Oceans (1978–2012) 102 (C3), 5829–5849.

Wahle, K., Stanev, E., 2011. Consistency and complementarity of different coastal ocean observations: A neural network-based analysis for the german bight. Geophysical Research Letters 38 (10).

Walker, D. T., 2006. Assimilation of sar imagery in a nearshore spectral wave model. Tech. rep., DTIC Document.

Waters, J., Wyatt, L. R., Wolf, J., Hines, A., 2013. Data assimilation of partitioned hf radar wave data into wavewatch iii. Ocean Modelling 72, 17–31.

Zamani, A., Azimian, A., Heemink, A., Solomatine, D., 2010. Non-linear wave data assimilation with an ann-type wind-wave model and ensemble kalman filter (enkf). Applied Mathematical Modelling 34 (8), 1984–1999.

Zhang, Z., Li, C., Li, Y., Qi, Y., 2006. Incorporation of artificial neural networks and data assimilation techniques into a third-generation wind-wave model for wave forecasting. Journal of Hydroinformatics 7, 65–76.